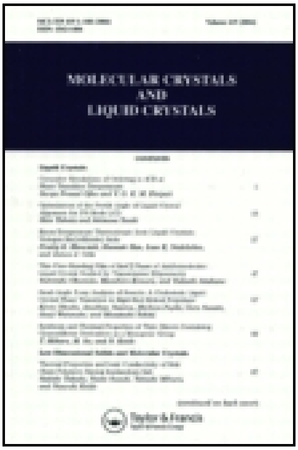

Molecular Crystals and Liquid Crystals
Publication details, including instructions for authors and subscription information:
http://www.tandfonline.com/loi/gmcl20

Structures and Physical Properties of Carbon Nanotube Reinforced PVDF Composites

Gwang Ho Kim [a] & Soon Man Hong [a]
[a] Polymer Hybrids Research Center, Korea Institute of Science and Technology(KIST), Seongbuk, Seoul, Korea

To cite this article: Gwang Ho Kim & Soon Man Hong (2007): Structures and Physical Properties of Carbon Nanotube Reinforced PVDF Composites, Molecular Crystals and Liquid Crystals, 472:1, 161/[551]-169/[559]

To link to this article: http://dx.doi.org/10.1080/15421400701545494

Mol. Cryst. Liq. Cryst., Vol. 472, pp. 161/[551]–169/[559], 2007
Copyright © Taylor & Francis Group, LLC
ISSN: 1542-1406 print/1563-5287 online
DOI: 10.1080/15421400701545494

Structures and Physical Properties of Carbon Nanotube Reinforced PVDF Composites

Gwang Ho Kim
Soon Man Hong
Polymer Hybrids Research Center, Korea Institute of Science
and Technology(KIST), Seongbuk, Seoul, Korea

Semicrystalline Poly(vinylidene fluoride)(PVDF)/Multi-walled carbon nanotube (MWNT) blends were melt compounded in an internal mixer. The relationships between structures and physical properties of PVDF/MWNT blends were studied. With increasing the content of MWNT, the apparent supercooling required for PVDF crystallization and the size of spherulites in PVDF were decreased. MWNT can be used as a nucleating agent. In the crystalline structures, the incorporation of MWNT produced a polar β-form crystal of PVDF. The permittivity of PVDF/MWNT blends was increased with increasing the MWNT content. The critical conductivity saturation point for the electrical conductivity in PVDF/MWNT blends was confirmed. Similar tendency was also observed in thermal conductivity.

Keywords: electrical conductivity; permittivity; poly(vinylidene fluoride); spherulite

INTRODUCTION

It is well known that CNTs are a kind of tubular carbon nanofiber (CNT) and have unique physical properties including high electrical conductivity and physical properties due to their high aspect ratio. This great aspect ratio may give rise to a high degree of specific surface area between polymer and inorganic Multi-walled carbon nanotube (MWNT), leading to high electrical conductivity and barrier properties [1,2]. Especially, incorporation of conductive filler such as

This study was supported by the 21 C Frontier R&D Program, Industrial Waste Recycling R&D Center.

Address correspondence to Dr. Soon Man Hong, Polymer Hybrids Research Center, Korea Institute of Science and Technology, 39-1 Hawolgok, Seongbuk, Seoul 136-791, Korea. E-mail: smhong@kist.re.kr

MWNT into the organic polymers including such as polyethylene [3], poly(methyl methacrylate) [4], polyacrylonitrile [5,6], polypropylene [7] holds promise for preparing an important class of new high performance hybrid materials [8–10].

In this study, the relationships between structures and physical properties based on semicrystalline PVDF and MWNT by melt compounding were investigated.

EXPERIMENTAL

Materials

A semicrystalline Poly(vinylidene fluoride) (PVDF), Solef 1010 of solvay Inc (Belgium), was used as a matrix resin. Multiwalled-carbon nanotube (MWNT; purity = 95%, average diameter = $10 \sim 15\,\text{nm}$, length = $10 \sim 20\,\mu\text{m}$) used as a dispersing agent, was supplied from Iiljin, Inc. (Korea). Pristine MWNTs were heated up to 550°C in air and held at 550°C for 1 hr. PVDF resin was also vacuum dried at 80°C for 24 hr prior to melt mixing. PVDF and MWNT were dry mixed via tumbling in a bottle, and then the mixture was melt-blended in an internal mixer (Haake Rheomix 600) for 10 min at 220°C at a rotor speed of 60 rpm. The contents (X) of PVDF/MWNT blends ranged from 0.01 to 5 wt%, and they were coded PVDF-X.

Measurement of Physical Properties

The thermal properties of PVDF/MWNT blends were investigated using differential scanning calorimeter (DSC 2010; TA instrument, Dupont) in a nitrogen atmosphere. Heating or cooling scan was performed at 10°C/min. The samples were held at 220°C in the molten state for 5 min to eliminate the thermal history prior to cooling scan. The polarized optical texture of PVDF/MWNT blends were observed by a Leitz Ortholux II microscope equipped with a heating stage and a programmable PID temperature controller model 350. The radial growth rate of PVDF resin was observed by the same microscope. Wide angle X-ray diffraction (WAXD) experiment was carried out by a Rigaku Denki with Ni-filtered CuKα radiation at 40 kV and 100 mA. Scanning was performed at a scan rate of 5°/min. Field emission scanning electron microscopic (FESEM; JEOL, JSM-6340F) observations were carried out on the surface of PVDF/MWNT blends. The surfaces of the samples were sputter-coated with a thin gold layer prior to scanning.

Dielectric measurements were performed on a frequency response analysis system using dielectric analyzer (Novocontrol GmbH, Germany) with a frequency range from 10^{-1} to 10^{4} KHz. Electrical conductivity measurement was performed using the four-probe method to eliminate the effect of contact resistance. A Keithley 2400 digital multimeter equipped with a YEW 2553 DSC DC voltage current standard (YEW Electronics, Japan) was used to measure the I-V characteristics of the samples at room temperature. Thermal conductivity was measured using TC probe (Mathis Instrumental Ltd).

RESULTS AND DISCUSSION

The thermomechanical properties of semicrystalline polymers are highly dependent on the processing conditions which governs the crystallization process. Much effort has been made to describe the crystallization kinetics and morphology of semicrystalline polymer [11–13]. In general, crystallization proceeds via homogeneous and/or heterogeneous nucleation, followed by the growth of the nucleated spherulites. Nucleating agents include inorganic additives such as talc, chalk, glass, silica and MWNT. It has been fairly well recognized that the presence of a nucleating agent has a profound influence on the crystallization kinetics of semicrystalline polymer [11–13]. The higher crystallization rate by incorporating a nucleating agent improves productivity by shortening the molding cycle. Further, it leads to heterogeneous nucleation and consequently enhances the physical properties of the molded parts by developing finer grain structure [14]. Figure 1

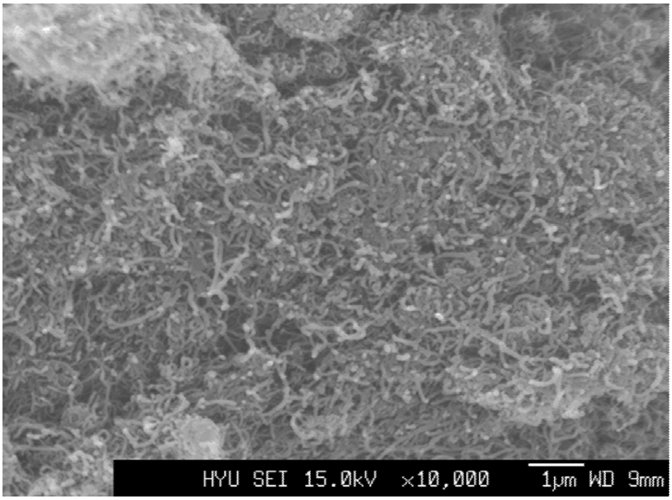

FIGURE 1 FESEM micrographs of pristine MWNT.

shows the FESEM micrographs of pristine MWNT used as a nucleating agent in PVDF matrix. MWNT exhibits highly curved and random coiled features, which may be attributed to hydrogen bonding and van der Waals attractive interactions between carbon nanotubes [15,16].

Crystallization behaviors of PVDF/MWNT blends can be seen by observing the crystal morphology. Using the polarized optical microscope equipped with a hot stage, crystal morphology and radial growth behavior of spherulites were observed. Figures 2–4 show the polarized optical micrographs of PVDF/MWNT blends, isothermally crystallized at 160°C. The morphologies are totally different from each other. Figures 2–4 show a well developed spherulite, later limited by several adjacent ones, typical crystalline structure of PVDF. Grain spherulitic structures containing a nucleated PVDF are observed with increasing the content of MWNT and crystallization time. This means that MWNT can be used as a nucleating agent in PVDF matrix. The melt crystallization exotherms of PVDF and PVDF/MWNT blend systems were observed during the cooling stage, as shown in Table 1. The melt crystallization temperature (Tmc) of PVDF increased with increasing the MWNT content because the MWNT phases dispersed finely within the PVDF matrix promotes heterogeneous nucleation [11,12]. The gradual decrease in apparent supercooling ($\Delta T = T_p - T_o$; T_p is the melting peak temperature and T_o is the onset temperature of crystallization) further supports the validity of this explanation. The apparent supercooling required for initiating crystallization was 24°C for pure PVDF. However, it decreased to 20.3°C with increasing the MWNT content as shown in Table 1 [13,14].

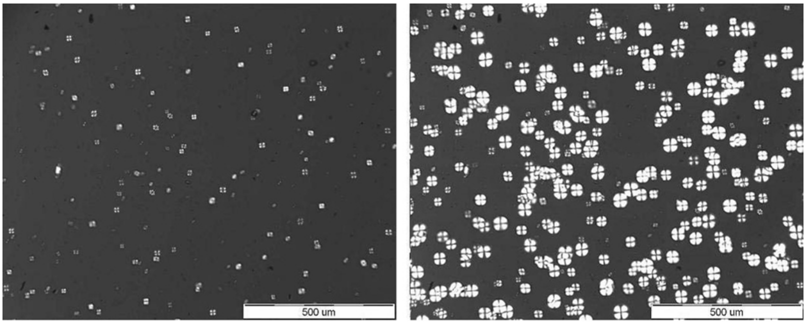

(a) (b)

FIGURE 2 Polarized optical micrographs of PVDF resin taken during isothermal crystallization at 160°C after different crystallization times (a) 11 min (b) 20 min.

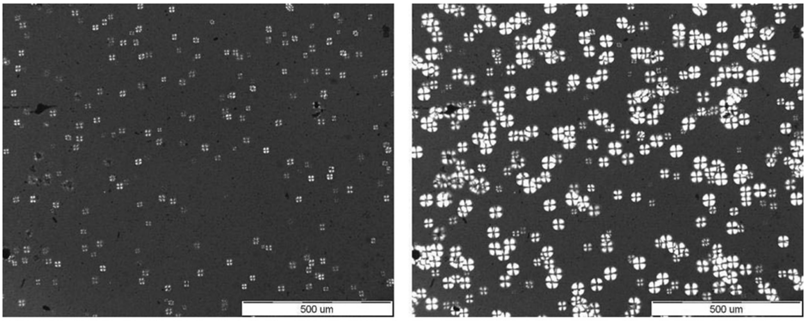

(a) (b)

FIGURE 3 Polarized optical micrographs of PVDF/MWNT blends with 0.05 wt% MWNT during isothermal crystallization at 160°C after different crystallization times (a) 11 min (b) 20 min.

WAXD profiles of PVDF and PVDF/MWNT composite are shown in Figure 5. Within a given range of scattering angle, three characteristic diffraction peaks appear at $2\theta = 17.7$, 18.4, and 19.9°, which correspond to (100), (020), and (110) reflections, respectively. This is assigned to the α-phase crystal which has a non-polar trans-gauche-trans-gauche (TGTG) conformation. PVDF/MWNT blends exhibit decreased peaks for α-phase crystal from 0.5 wt% loading. In addition to the features associated with α-phase crystal, the introduction of MWNT produces a shoulder at a 2θ value of 20.7° and it is clearer with increasing the MWNT content. This is attributed to the formation of β-phase crystal which has all-trans conformation. It is recognized that

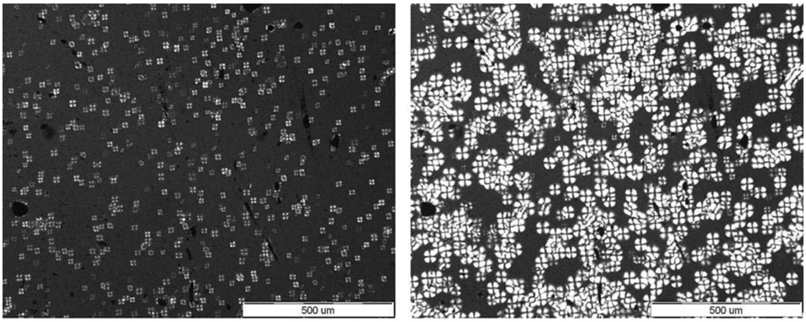

(a) (b)

FIGURE 4 Polarized optical micrographs of PVDF/MWNT blends with 0.1 wt% MWNT during isothermal crystallization at 160°C after different crystallization times (a) 11 min (b) 20 min.

TABLE 1 Thermal Properties of Several PVDF/MWNT Blends

CNT %	Tm^{a} °C	Tm^{b} °C	Tmc^{a} °C	Tmc^{c} °C	$\Delta\mathrm{T}^{d}$ °C
0	172.3	177.9	142.4	148.3	24.0
0.01	172.5	178.5	142.4	148.6	23.9
0.1	172.6	178.8	142.4	148.8	23.8
0.5	172.6	180.0	145.8	151.1	21.5
1	172.6	181.1	146.8	151.6	21.0
3	172.8	181.4	147.8	152.4	20.4
5	173.1	182.1	147.9	152.8	20.3

^{a}Peak temperature.
^{b}Offset temperature on the heating scan.
^{c}Onset temperature on the cooling scan.
$^{d}\Delta$T, degree of supercooling.

the β-phase, the most polar among other crystals, exhibits piezoelectric, pyroelectric, and ferroelectric properties and it is typically obtained by stretching and electric polling [17]. This implies that the incorporation of alien particle can be considered as a method to increase those properties of PVDF.

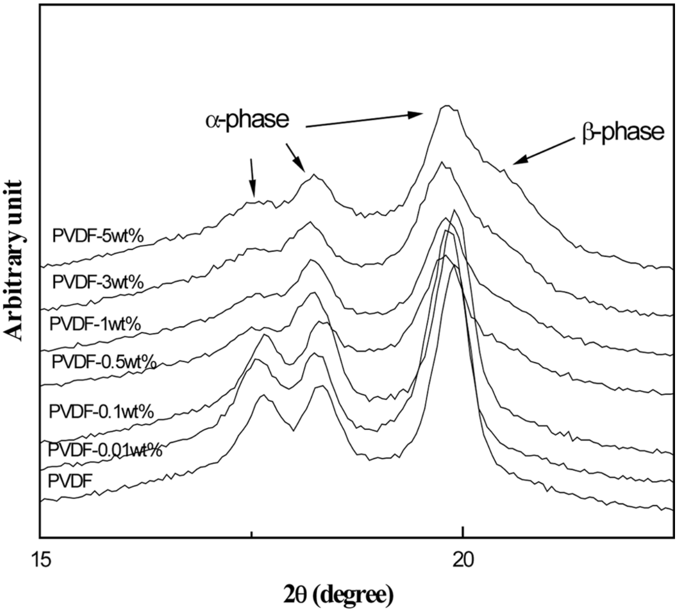

FIGURE 5 WAXD patterns of PVDF and PVDF/MWNT blends.

It is well known that dispersion state of MWNT in the polymer matrix directly affects the physical properties of PVDF/MWNT blends. We herein investigated the effect of MWNT content on the permittivity, electrical conductivity and thermal conductivity of PVDF. The variations in permittivity of the PVDF/MWNTs blends are given in Figure 6 as a function of the MWNTs content. The permittivity of the PVDF blends is proportionally dependent on the content of MWNTs. Permittivity is improved with increasing the content of MWNT. However, permittivity is decreased with increasing the frequency in the range from 10^{-1} to 10^4 KHz. Ionic conduction phenomena are slightly observed above 5 wt% of MWNT. These results implied obviously that the PVDF resin filled with MWNTs could be prospective EMI shield material since we can enhance the permittivity and conductivity by controlling the content of MWNT. Figure 7 shows the variations of the electrical conductivity of PVDF blends with the MWNT contents (conductivity of MWNT:75 S/cm). PVDF is not an electrically conductive polymer showing the conductivity in dry state as low as 10^{-14} S/cm.

The electrical conductivity was increased from 10^{-14} to 10^0 S/cm with increasing the content of MWNT from 0 to 5 wt%. However, when the content of MWNTs went over 5 wt%, the electrical conductivity

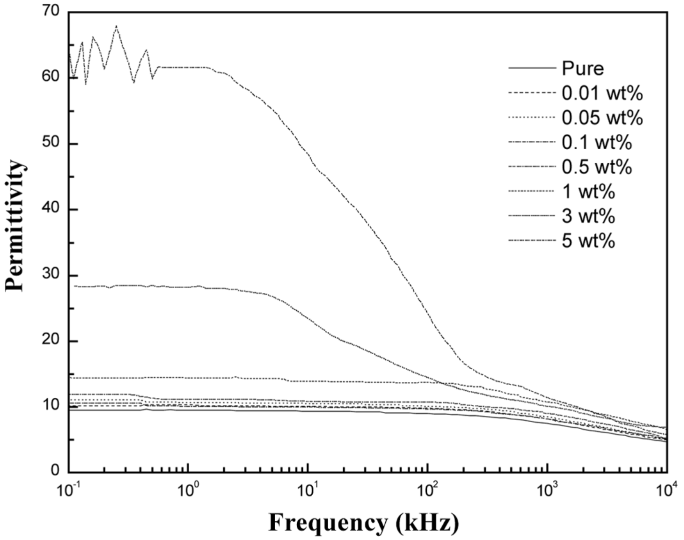

FIGURE 6 Variation of the permittivity of PVDF and PVDF/MWNT blends with MWNT content.

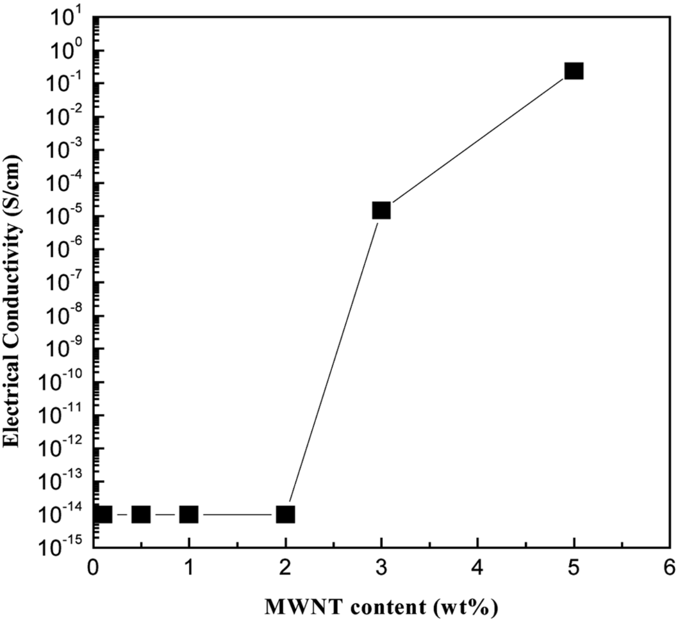

FIGURE 7 Variation of the electrical conductivity of PVDF and PVDF/MWNT blends with MWNT content.

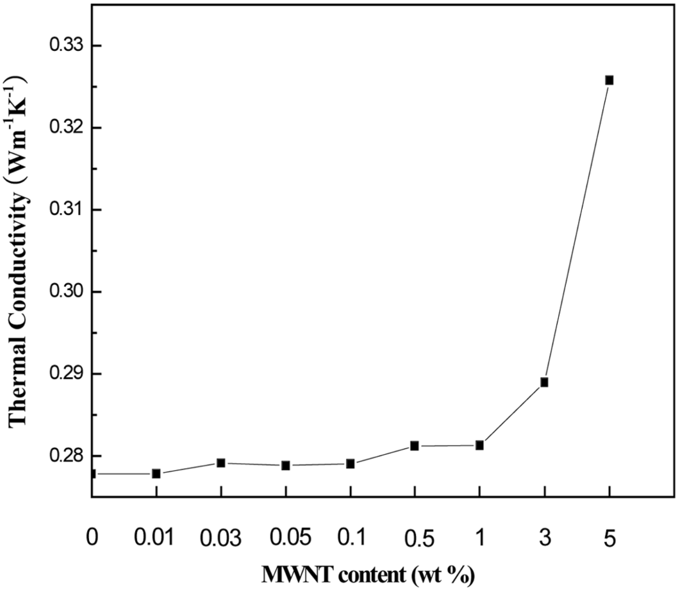

FIGURE 8 Variation of the thermal conductivity of PVDF and PVDF/MWNT blends with MWNT content.

was almost independent of the MWNTs content. This indicates that there is conductivity saturation point from a critical content [18]. Further incorporation of MWNT does not significantly alter the electrical conductivity. Similar tendency was also observed in thermal conductivity above 3 wt% of MWNT, as shown in Figure 8.

CONCLUSIONS

We have investigated the relationships between structure and physical properties of PVDF/MWNT blends by melt compounding. With increasing the MWNT content, supercooling required for PVDF crystallization and the size of spherulites in PVDF decrease. MWNT can be used as a nucleating agent of PVDF. The incorporation of MWNT produced a polar β-form crystal of PVDF. The permittivity, electrical conductivity and thermal conductivity was increased with increasing the MWNT content. The critical conductivity saturation point and percolation threshold for the PVDF/MWNT were also observed. Thus, PVDF/MWNT blends are expected to be used extensively in piezoelectric and pyroelectric applications.

REFERENCES

[1] Treacym, M. J., Ebbsen, T. W., & Gibson, J. M. (1991). *Nature*, *381*, 678.
[2] Ma, R. Z., Wu, J., Wei, B. Q., Liang, J., & Wu, D. H. (1998). *J. Mat. Sci.*, *33*, 5243.
[3] Zou, Y., Feng, Y., Wang, L., & Liu, X. (2004). *Carbon*, *42*, 271.
[4] Jin, Z., Pramoda, K. P., Xu, G., & Goh, S. H. (2001). *Chem. Phys. Lett.*, *337*, 43.
[5] Min, B. G., Sreekumar, T. V., Uchida, T., & Kumar, S. (2004). *Carbon*, *43*, 599.
[6] Guo, H., Sreekumar, T. V., Liu, T., Minus, M., & Kumar, S. (2005). *Polymer*, *46*, 3001.
[7] Kearns, J. C. & Shambaugh, R. L. (2002). *J. Appl. Polym. Sci.*, *86*, 2079.
[8] Quan, D., Dickey, E. C., Andrews, R., & Rantell, T. (2000). *Appl. Phys. Lett.*, *76*, 2868.
[9] Shaffer, M. S. P. & Windle, A. H. (1999). *Adv. Mater.*, *11*, 937.
[10] Zhang, X., Liu, T., Sreekumar, T. V., Kumar, S., Moore, V. C., Hauge, R. H., & Smalley, R. E. (2003). *Nano Lett.*, *3*, 1285.
[11] Hong, S. M., Kim, B. C., Kim, K. U., & Chung, I. J. (1992). *Polymer J.*, *24*, 727.
[12] Desio, G. P. & Rebenfeld, L. (1990). *J. Appl. Sci.*, *39*, 825.
[13] Nadkarni, V. M. & Jog, J. P. (1986). *J. Appl. Polym. Sci.*, *32*, 5817.
[14] Lee, Y. & Porteer, R. S. (1986). *Polym. Eng. Sci.*, *26*, 633.
[15] Ebbesen, T. (1997). *Carbon Nanotubes; Preparation and Properties*, CRC Press: New York.
[16] Li, S. N., Li, Z. M., Yang, M. B., Hu, Z. Q., & Huang, R. (2004). *Mater. Lett.*, *58*, 3967.
[17] Furukawa, T., Data, M., & Fukada, E. (1980). *J. Appl. Phys.*, *51*, 1135.
[18] Kotsilkova, R., Nesheva, D., Nedkov, I., Krusteva, E., & Stavrev, S. (2004). *J. Appl. Polym. Sci.*, *92*, 2220.